

## Original Article

# Adenanthin induces G2/M arrest and apoptosis in human non-small-cell lung cancer cells

Anbang Hu<sup>2\*</sup>, Jinping Li<sup>2</sup>, Yulin Fang<sup>3</sup>, Weiqing Li<sup>1\*</sup>

<sup>1</sup>Department of Traditional Chinese Medicine, Luohu District People's Hospital, Shenzhen 518020, China;

<sup>2</sup>Department of Internal Medicine, Luohu District Chinese Medicine Hospital, Shenzhen 518021, China;

<sup>3</sup>Comprehensive Department of Affiliated Hospital of Jiangnan University, Wuhan 430015, China. \*Equal contributors.

Received August 2, 2018; Accepted October 10, 2018; Epub March 15, 2019; Published March 30, 2019

**Abstract:** *Background:* Non-small cell lung cancer (NSCLC) is a frequently encountered primary malignancy that is often immune to conventional chemotherapy. New chemotherapeutic agents are vital in combating this increasingly problematic disease. A natural diterpenoid derivative extracted from *Isodon adenanthus* leaves, adenanthin, has been demonstrated to produce anti-leukemic activity by acting on peroxiredoxin I/II. However, its role in NSCLC has yet to be fully investigated. *Methods:* Colony formation assays and CCK-8 assays were employed to investigate the growth of NSCLC cells and healthy cells. Induction of cellular apoptosis or arrest of cell cycles were determined by flow cytometric analysis, based on the Hoechst 33342 staining method or annexin V/propidium iodide. Intracellular levels of proteins related to apoptosis and the cell cycle were quantified via Western blot assay. A pan-caspase inhibitor, Z-VAD-FMK, allowed blockage of caspase activity in NSCLC (A549 and H460) cells, prior to treatment with adenanthin. Nude mice xenografts were created by subcutaneous inoculation, allowing researchers to study the *in vivo* effects of adenanthin (20 mg/kg, 40 mg/kg) on H460 cells. Apoptosis from mice tissues was observed by TUNEL assay. Pathological histology of tumor tissues was detected by H & E staining. *Results:* NSCLC cells (A549 and H460) were particularly sensitive to the effects of adenanthin. Adenanthin also conferred minimal cytotoxic damage to healthy cells. Adenanthin blocked NSCLC cell proliferation by arresting cell cycle progression in the G2/M phase and caspase3-dependent apoptosis. Adenanthin was able to attenuate tumor growth in mouse xenograft models while being well-tolerated, having an overall effect of prolonging mice survival. *Conclusion:* Adenanthin may serve as a novel anti-cancer agent that is potent and selective in eliminating NSCLC tumor cells.

**Keywords:** NSCLC, adenanthin, caspase3, apoptosis

## Introduction

Lung malignancies have become increasingly common, worldwide. They confer a high rate of mortality and represent a primary cause of cancer-associated deaths in both genders across several countries [1]. Of all histological types, non-small cell lung cancer (NSCLC) represents the most numerous subtype, accounting for about 85% of all lung cancer cases [2]. The gold standard management regimen of NSCLC patients includes a combination of chemotherapy, radiotherapy, and surgery [3]. However, despite astounding developments in all three treatment modalities, patients with NSCLC still face a dismal five-year survival rate of less than 20% [4]. Part of the high mortality rate can be

attributed to severe chemotherapeutic drug toxicity and resistance. Efforts to overcome these hurdles have given rise to biological agents that target specific molecules in the cancer cascade. For example, NSCLC patients that have epidermal growth factor receptor (EGFR) mutations are treated with tyrosine kinase inhibitors (TKIs) [5, 6]. However, overall patient survival still remains low.

Traditional Chinese herbal agents often consist of a number of natural compounds that are biologically active. These agents have been touted to possess impressive therapeutic efficacy accompanied by minimal adverse effects. These claims have fueled research in developing first-line chemotherapeutic agents based

## Adenanthin inhibits non-small-cell lung cancer cell growth

on these compounds [7, 8]. Mechanistic insight has revealed that these agents are potent inducers of apoptosis and immune activation, both of which are thought to contribute to restriction of tumor growth [9, 10]. Adenanthin is a traditional Chinese herb, a diterpenoid compound isolated from leaves of *Isodon adenanthus*. Accumulating evidence has indicated that the *Isodon* species possesses a broad spectrum of pharmacological effects that includes antioxidant activity [11, 12], anti-bacterial infections [13], anti-inflammation [14], and anti-cancer activity [15]. Its bioactive components are known as diterpenoids [16], which are a large and structurally diverse class of secondary metabolites [17, 18]. Therefore, it is necessary and vital to explore the biological activities and underlying targets of diterpenoids. However, the underlying mechanisms of the natural compound adenanthin in its ability to inhibit human NSCLC cells and tumor bearing mice models have not yet been investigated.

Collectively, the present study demonstrates that NSCLC cells are especially vulnerable to the effects of adenanthin, in contrast to other types of cancer cells. Adenanthin induces apoptosis by inhibiting the caspase3-dependent pathway and stops cell proliferation by halting the cell at the G2/M phase of the cell cycle. Adenanthin can attenuate NSCLC cell growth *in vitro* as well as shrink xenograft tumors on mice models *in vivo*. These pre-clinical results document the potential anti-tumor properties of adenanthin in NSCLC.

### Materials and methods

#### *Drugs and reagents*

Adenanthin was purchased from Faces Biochemical Com., Ltd (Wuhan, Hubei, China; catalogue no. CFN99215) and stock solutions of 40 mM (20 mg/mL) were prepared by dissolving the compound in DMSO (Sigma-Aldrich, St. Louis, MO). HPLC analysis confirmed that its purity was at least 95%.

Rhodamine 123 and Hoechst 33342 were bought from Sigma-Aldrich (MO, USA). Cell Counting Kit-8 (CCK-8) and the Annexin V/PI apoptosis kits were procured from the Dojindo Laboratories (Japan) and Invitrogen (CA, USA), respectively. Antibodies against CDK2, Cyclin

B1, and  $\beta$ -actin were bought from Epitomics (CA, USA). Ki67 antibodies were procured from Santa Cruz (CA, USA). Anti-Bcl-2, Bad, Bax, cl-caspase3 (Asp175), caspase3, cl-PARP, PARP, cytochrome C, and GAPDH were all obtained from Cell Signaling Technology (MA, USA). Terminal deoxynucleotidyl transferase (TdT) dUTP nick-end labeling (TUNEL) assay kit was obtained from Abcam (Cambridge, England). Chem Mate En Vision Kit was purchased from Dako (Glostrup, Denmark).

#### *Cell lines and cell cultures*

All three cell lines, BEAS-2B, H460, and A549, were obtained from the Cell Bank of Type Culture Collection of the Chinese Academy of Sciences (Shanghai, China). A549 and H460 cells were cultured in DMEM medium (Gibco, NY, USA) and RPMI-1640 (Gibco, NY, USA), respectively. Both mediums were supplemented with 10% fetal bovine serum (Gibco) that contained 100 U/mL penicillin-streptomycin (Hyclone, UT, USA). BEAS-2B cells were grown in LHC-8 medium (Gibco, NY, USA) added with 1% epidermal growth factor (Hyclone, UT, USA) and 10% fetal bovine serum (Gibco). All cell lines were incubated at 37°C and 5% CO<sub>2</sub>. Further explanations regarding other cell lines are disclosed in Additional File 1 ([Supplementary Material and Methods](#)).

#### *Cell viability assay*

Cell viability was quantified with the CCK-8 kit, in accordance with manufacturer instructions. Briefly, 96-well plates were utilized to seed cancer cells that were subsequently treated for 48 hours with adenanthin of increasing concentrations (0, 5, 10, 20, 40, 80, or 100  $\mu$ M). Additionally, adenanthin was also administered at different time points (0, 24, 48, or 72 hours). CCK-8 solution was mixed in after the stipulated time periods and left to incubate with cancer cells for 4 hours. Cell survival percentages were quantified by SpectraMax 190 microplate reader (Molecular Devices) based on the absorbance.

#### *Cell cycle and apoptosis analysis*

The proportion of cells in each stage of the cell cycle was measured using propidium iodide (PI) staining assay. Cancer cells were harvested after being exposed to various concentrations

## Adenanthin inhibits non-small-cell lung cancer cell growth

of adenanthin for 48 hours and fixed with 70% ethanol. Cells were subsequently centrifuged for 5 minutes at speeds of 3,000 rpm. Next, cells were incubated for 30 minutes with 100 mg/mL RNase in PBS at 37°C and stained with 50 mg/mL PI diluted in PBS. Cell Lab Quanta SC flow cytometer (Beckman Coulter, USA) was used to analyze cell cycle distribution.

The degree of cell apoptosis was analyzed using the Annexin V-FITC Apoptosis Detection Kit (BioVision).  $5 \times 10^5$  cells were first immersed in various concentrations of adenanthin. After 48 hours, cells were resuspended with 500 mL of binding buffer before being incubated with PI (5 mL) and Annexin V-fluorescein isothiocyanate (FITC; 5 mL). After 30 minutes, fluorescence-activated cell sorting (FACS) by flow cytometer (Becton Dickinson) was used to analyze cells. Cells that were only stained with Annexin V-FITC were interpreted as having gone through early apoptosis while cells that stained both with Annexin V-FITC and PI were combined for analysis.

### *Colony formation assay*

Six-well plates were used to seed cancer cells at a density of 500 cells per well. All wells were given different concentrations of adenanthin (0  $\mu$ M, 20  $\mu$ M) and left for 48 hours [19]. Post-treatment, cells were left alone for one week to encourage colony formation. All cells were then fixed with 4% paraformaldehyde and subjected to 0.1% crystal violet staining. After staining, cells were subjected to three washings and air-drying before being quantified and photographed under a microscope (Leica, Germany).

### *Hoechst staining*

Hoechst 33342 was used to identify morphological changes in nuclear organization for determining apoptotic cells, as described previously. Wavelengths of 490/540 nm were used to acquire cell images. The membrane potential of mitochondria was estimated by the relative ratio between the absorbance at 590 nm and 540 nm.

### *Mitochondrial membrane potential ( $\Delta\Psi_m$ ) assay*

Changes in mitochondrial membrane potential were determined by staining 20  $\mu$ M adenanthin

cells with JC-1. Changes were quantified using wavelengths of 490/540 nm. The mitochondrial membrane potential was derived from the ratio between 590 nm (red signal) and 540 nm (green signal).

### *Western blot analysis*

Multiple concentrations of adenanthin (0  $\mu$ M, 20  $\mu$ M) were used to treat A549 and H460 cancer cells for 48 hours. Cell lysates were then prepared, followed by protein separation utilizing SDS-PAGE gel. Gel slices were then relocated onto polyvinylidene difluoride (PVDF) membranes (Millipore, Bedford, MA, USA). Blocking of endogenous reactions was done, followed by specific antibody probing. All membranes were then incubated with horseradish peroxidase-conjugated goat anti-Rabbit IgG after washing. They were visualized utilizing the enhanced chemiluminescent (ECL) detection reagent from Pierce (Rockford, IL, USA) [20].

### *Animal treatment with adenanthin*

Six-week old 18 g nude mice were obtained from Shanghai SLAC Laboratory Animal (China). All animal experiments were carried out in strict compliance to the National Institutes of Health Guide for the Care and Use of Laboratory Animals, while experimental animal protocols were pre-approved by the Institutional Animal Care and Use Committee of Luohu District People's Hospital. Upon arrival at the facility, mice were initially reared in pathogen-free environment for one week. All mice received inoculation of  $2 \times 10^6$  H460 cells in 100  $\mu$ l PBS at their left flank. The mice were then randomly grouped into three groups, consisting of 5 mice each, after one week. Each group received daily intraperitoneal injections of either PBS (control group), 20 mg/kg of adenanthin, or 40 mg/kg of adenanthin. After 4 weeks of treatment, all mice were anesthetized with isoflurane delivered by a R550 multi-channel small animal anesthesia machine (Ruiwode Lift Technology, Shenzhen, China) and sacrificed in a CO<sub>2</sub> chamber to harvest liver and tumor specimens, as well as weights of the tumors.

### *Immunohistochemistry*

All tumors were sectioned into 4 mm-thicknesses before being formalin-fixed and embedded with paraffin. Antibodies against CKD2, Ki67,

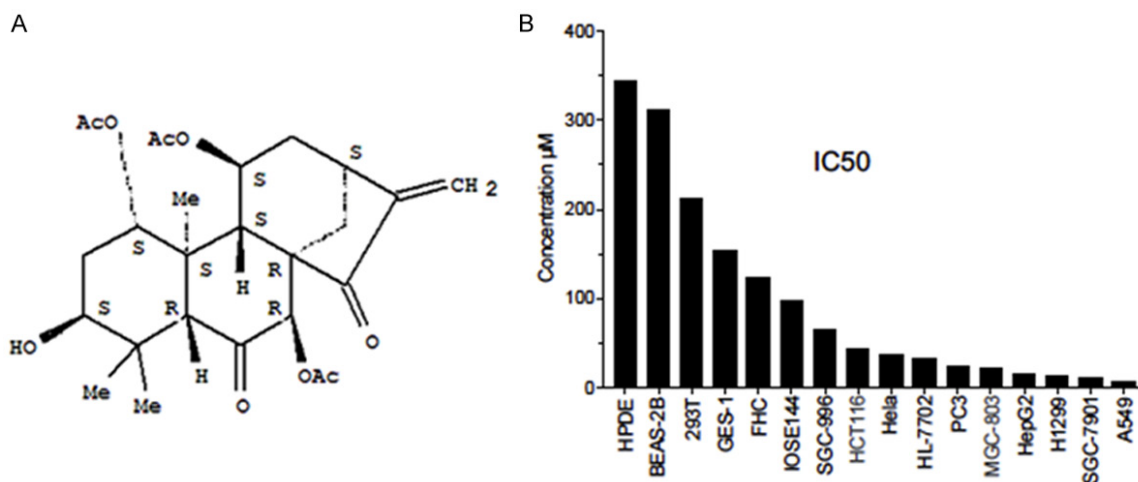


**Figure 1.** Highly specific and targeted cytotoxic effects of adenanthin on cancer cells. A. Adenanthin biological structure. B. Adenanthin IC<sub>50</sub> in a variety of cancer cells and healthy cells. Normal cells, including human colon epithelial cell (FHC), human pancreatic ductal epithelial cell (HPDE), human gastric epithelial cells (GES-1), human embryonic kidney (HEK) 293T, immortalized human bronchial epithelial cells (BEAS-2B), human ovarian epithelial cells (IOSE144), human hepatic immortal cells (HL-7702), and different human cancer cell lines were subjected to a 48 hour exposure to 0-400 µmol/L of adenanthin. The CCK8 assay quantified degree of cytotoxicity. All results are based on a minimum of 3 independent experiments.

and TUNEL were first used to stain slides prior to a second staining with secondary antibodies. Slides were then visualized with the Chem Mate En Vision Kit (Dako, Glostrup, Denmark) and analyzed at  $\times 400$  magnification under a microscope. H & E staining was carried out for a few slides for histological analysis (Sigma-Aldrich, MO, USA). TUNEL assay was performed on selected slides, which were then subjected to *in situ* cell death detection analysis using a kit (Abcam, Cambridge, England).

#### Statistical analysis

All results are interpreted as mean  $\pm$  S.D. Student's t-test was used to detect significant differences between the two groups. All data was analyzed with the assistance of the SPSS program, version 18.0 (SPSS, Chicago, IL, USA). *P* value < 0.05 indicates statistical significance.

#### Results

##### *Adenanthin possess potent tumor-eliminating properties and is extremely toxic to NSCLC cells*

Adenanthin is an extract of *Isodon adenanthus* leaves and is a monomeric diterpenoid in nature (Figure 1A). Modern pharmacologic methods indicate that this compound is able to

exert strong cytotoxic effects onto malignant cells. Present experiments comprised of a cell-based screening, aiming to investigate how adenanthin affected the viability of various types of healthy cells and tumor cells (Figure 1B). Nine human cancer cell lines and 7 healthy cell lines were incubated for 48 hours with increasing concentrations of adenanthin (0-400 µmol/L). CCK-8 assay evaluated the viability of the tested cells. Remarkably, adenanthin was able to inhibit the growth of human prostate, gallbladder, colon, gastric, liver, pancreatic, and cervical carcinoma cells at IC<sub>50</sub> values ranging between 20 µmol/L to 200 µmol/L. NSCLC cells were noted to be exquisitely vulnerable to the deleterious effects of adenanthin. In contrast, adenanthin demonstrated comparatively reduced cytotoxicity in the presence of normal human bronchial epithelial cells (BEAS-2B), implying its selectivity for malignant cells.

##### *Adenanthin inhibits NSCLC cell growth in both a dose-dependent and time-dependent manner*

To measure adenanthin cytotoxicity on NSCLC cells, two human NSCLC cell lines (A549 and H460) and a normal human bronchial epithelial cell line (BEAS-2B) were exposed to different concentrations of adenanthin (0, 10, 20, 40, 80, or 100 µM) for varying durations (24, 48, or

## Adenanthin inhibits non-small-cell lung cancer cell growth

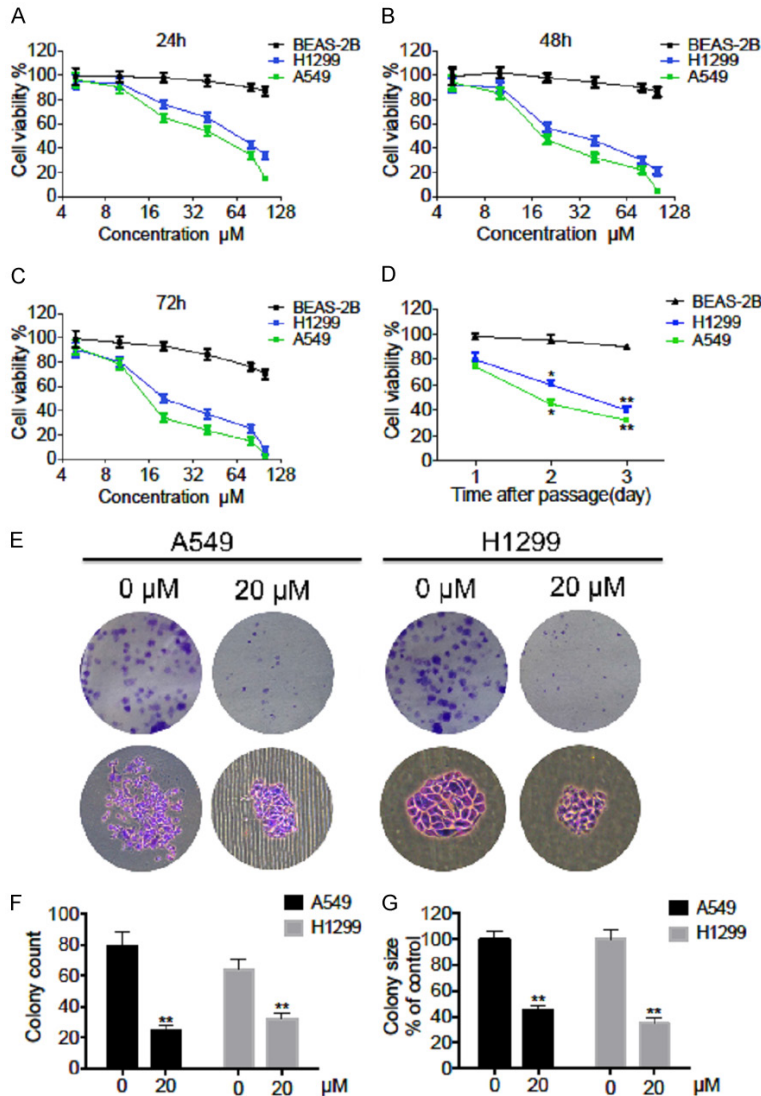


**Figure 2.** Adenanthin inhibits NSCLC cells growth in both a time- and dose-variant manner. A-C. Two NSCLC cancer cells (A549 and H460) and one normal human bronchial epithelial cell (BEAS-2B) were subjected to cell viability assays post-exposure to different concentrations of adenanthin that ranged from 0 µM to 100 µM. Controls were deemed to be cells treated with vehicle. All the cells were cultured for 24 hours, 48 hours and 72 hours. D. At a fixed dose (20 µM), adenanthin resulted in decreased viability of NSCLC cells (A549 and H460) and one normal human bronchial epithelial cell (BEAS-2B) in a time-dependent manner (24 hours, 48 hours, or 72 hours). E. Colony formation assays. A549 and H460 cells were administered with indicated doses of adenanthin. All colonies were stained with crystal violet for subsequent visualization. F. All formed colonies were counted manually for the colony formation assay. G. The colonies size were measured for the colony formation assay. \*,  $P < 0.05$ ; \*\*,  $P < 0.01$ .

72 hours). Subsequent CCK-8 assays revealed that adenanthin conferred its cytotoxic effects in a concentration- and time-dependent manner on multiple pancreatic cancer cell lines. In contrast, this compound had no marked effects on BEAS-2B cells (Figure 2A-D), further supporting the selectivity of adenanthin for

malignant cells. From initial cytotoxicity results, this study selected the doses 0 and 20 µM of adenanthin to proceed with further colony formation assays (Figure 2E). Increasing adenanthin doses was demonstrated to reduce cell colony numbers (Figure 2F, 2G). Current data indicates that pancreatic cancer cells are affected by adenanthin in a time- and dose-dependent manner.

### *Adenanthin induces G2/M phase cell cycle arrest in NSCLC cells*

To inspect whether adenanthin attenuates cell growth by interfering with cell cycle progression, cell distribution in the cell cycle was quantified, as well as related cell cycle checkpoint factors. Results revealed that a 48-hour treatment period with 20 mM adenanthin treatment led to an increased number of cells in the G1 phase (Figure 3A, 3B). Adenanthin treatment raised the population of G1 phase cell from 46.23% (control) to 58.67% in A549 cells and from 42.56% (control) to 55.16% in H460 cells, both of which translates to an approximate 1.3-fold increase. Additionally, Western blot analysis demonstrates that adenanthin treatment lowered expression of CDC25C, Cyclin B1, and CDK2 (Figure 3C). Taken together, adenanthin can carry out its anti-proliferative effects by halting cells in the G1 phase of the cell cycle.

### *Adenanthin induces mitochondrial-related apoptosis in NSCLC cells*

This study evaluated the pro-apoptotic ability of adenanthin in NSCLC cells. Quantitative assessment of cell apoptosis was carried out using a dual-staining method with Annexin

## Adenanthin inhibits non-small-cell lung cancer cell growth

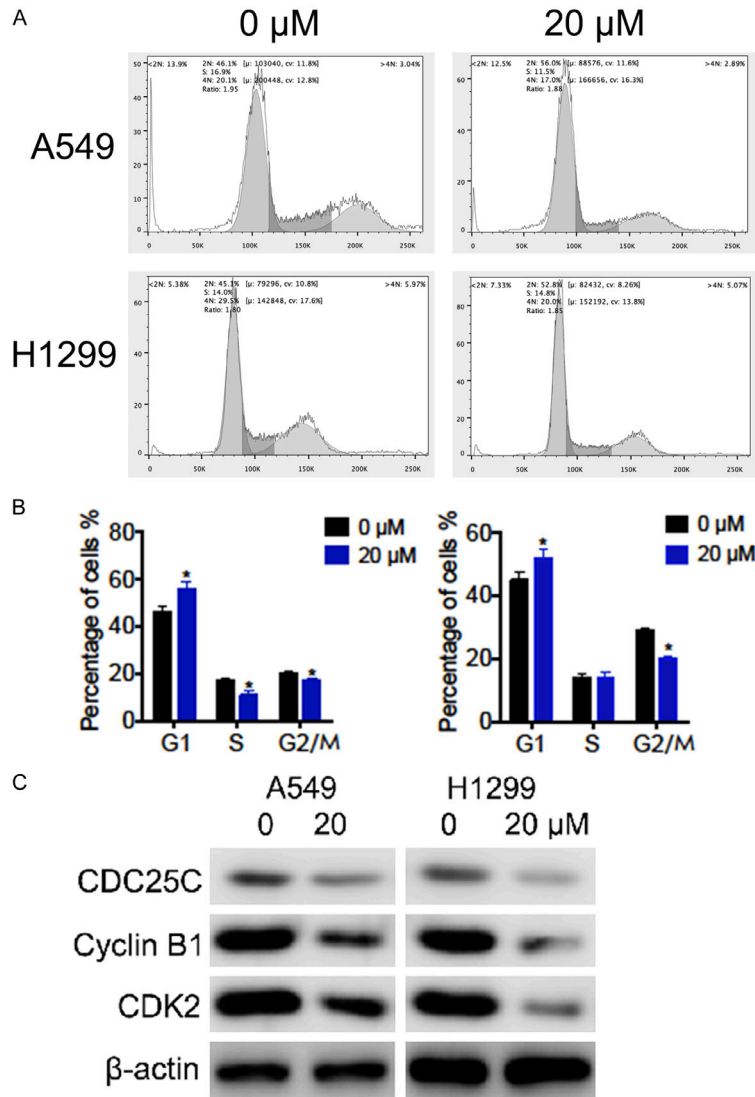


**Figure 3.** Adenanthin induced G1 phase cell cycle arrest in NSCLC cells. A, B. NSCLC cells were incubated in the presence of absence of 20 μM adenanthin for the specified times, prior to evaluating the proportion of cells in each phase of the cell cycle using flow cytometry. Proportions of each cell population is depicted as mean ± S.D. All results are based on a minimum of 3 independent experiments. \*, P < 0.05. C. Western blotting analysis of G1/S transition-related proteins after adenanthin treatment.

V-FITC and PI. Results revealed that a 48-hour treatment with 20 μM adenanthin was able to induce  $14.65 \pm 1.91\%$  and  $11.34 \pm 2.36\%$  apoptosis in A549 and H460 cells, respectively (Figure 4A). More extensive DAPI staining revealed nuclear fragmentation and condensation in the apoptotic cells (Figure 4B). This study further assessed changes in mitochondrial membrane potential ( $\Delta\Psi_m$ ), bcl-2 family proteins, cytochrome c release, proteolytic cleavage of procaspase, and the general cas-

pase inhibitor (z-VAD-fmk) rescue assay.  $\Delta\Psi_m$  reduction, as quantified by JC-1, was especially prominent in H460 cells that were exposed to 20 μM adenanthin (Figure 4C). z-VAD-fmk, an inhibitor of all cellular caspases, allowed researchers to determine if adenanthin also had the ability to block cell apoptosis through caspase-reliant methods. When z-VAD-fmk was added, the pro-apoptotic effects of adenanthin were attenuated, with only 3.53% of A549 cells shown to undergo apoptosis, compared to the previous value of 12.89%. Similarly, H460 cells underwent a decrease from 10.79 to 2332% (Figure 4D). Protein quantifications of A549 and H460 cells treated with 20 μM adenanthin, according to Western blotting analysis, showed that both cells had markedly decreased bcl-2 levels, while having increased bax levels. Increased levels of cytochrome c and increased cleavage of cl-PARP and procaspase-3 were also noted, suggesting the ability of adenanthin to activate intrinsic apoptosis pathways (Figure 4E).

### *Adenanthin attenuated in vivo tumor growth in vivo*

To assess the chemotherapeutic properties of adenanthin on growth of tumors *in vivo*,  $2 \times 10^6$  A549 cells were injected subcutaneously in the left flank of nude mice. Following the initial dose, all mice were given either 20 or 40 mg/kg of intraperitoneal adenanthin for 21 days. Adenanthin was able to significantly attenuate tumor growth (Figure 5A, 5B). Tumor masses in either group that received adenanthin treatment were markedly shrunken, in contrast to the control group (Figure 5C). IHC analysis of antigen identified by monoclonal antibody

## Adenanthin inhibits non-small-cell lung cancer cell growth

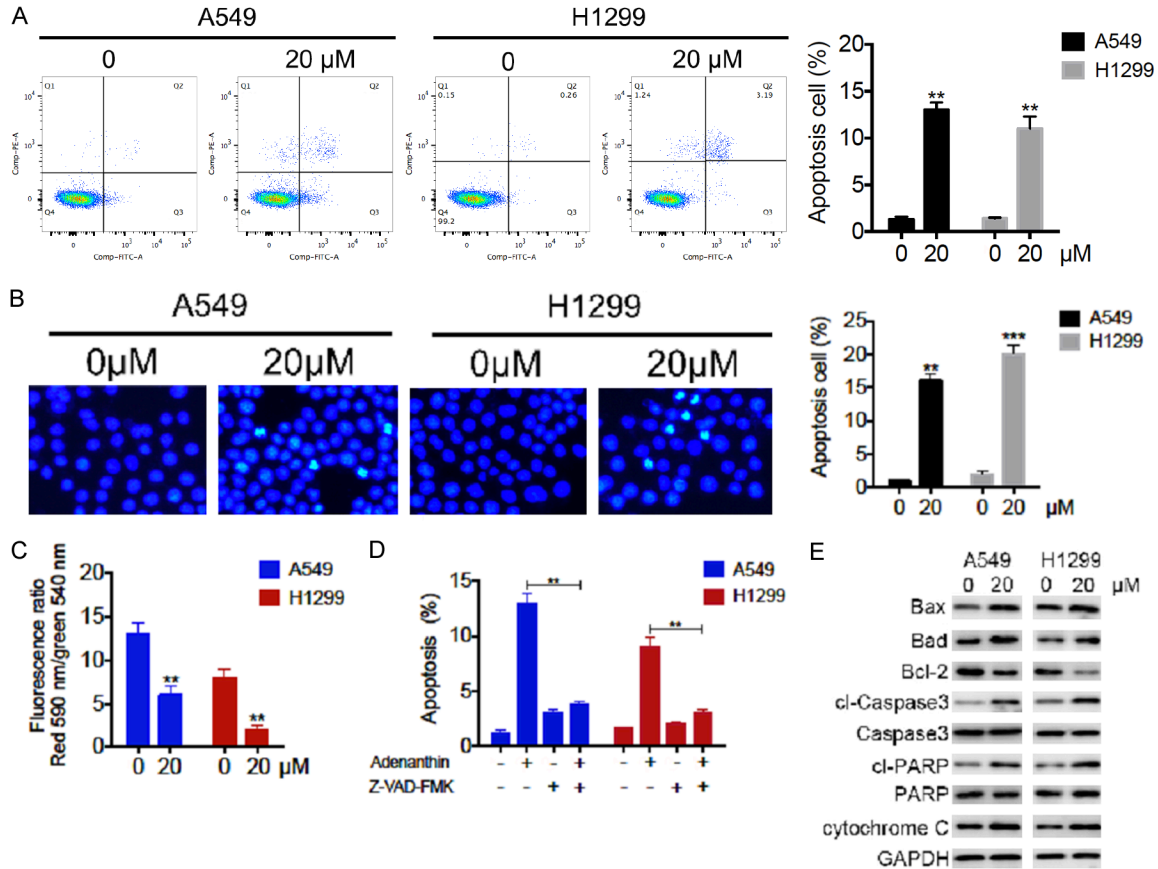


**Figure 4.** Adenanthin triggers mitochondrial-related apoptosis in pancreatic cancer cells. (A) Both A549 and H460 cells were scrutinized with flow cytometry and Annexin V-FITC/PI assay to determine the presence of apoptosis after being exposed to 20 μM adenanthin for 48 hours. Numbers indicate the percentage of cells in each quadrant. (B) DAPI staining allowed observation of cell morphology changes induced by adenanthin. Photomicrographs of cells in the control or 20 μM adenanthin treatment are shown. (C) JC-1 staining followed by flow cytometry were used to determine mitochondrial membrane potential ( $\Delta\Psi_m$ ). A loss of  $\Delta\Psi_m$  is denoted by a reduction in the ratio of FITC signals to PE signals (D) A549 and H460 cells that were first pretreated with 20 μM z-VAD-fmk, a pan caspase inhibitor, for 1 hour, were then incubated with 20 μM adenanthin for 48 hours. Flow cytometry was used to assess for apoptosis (E) Cytochrome c in cytosol and mitochondria, cleaved-PARP, cleaved-caspase-3, bcl-2, bad, and bax were quantified with Western blotting analysis after 20 μM adenanthin treatment for the stipulated durations. All results are based on a minimum of 3 independent experiments. Internal control was determined to be GAPDH. \*\*,  $P < 0.01$ ; \*\*\*,  $P < 0.001$ , versus the drug-untreated group.

(Ki67), which is associated with cellular proliferation, as well Cyclin-dependent kinase 2 (CDK2), were decreased in adenanthin-treated xenograft tumor tissues in addition to showing significantly fewer proliferative cells. Moreover, results of TUNEL assay revealed that TUNEL-positive cells were increased, indicating a higher proportion of apoptotic cells in adenanthin-treated tumors (Figure 5D). Furthermore, survival was remarkably prolonged in both adenanthin treatment groups (Figure 5E,  $P = 0.007$ ). Body weights and general appearances of each mouse were regularly monitored during the experiment. Both general appearances and body weights of mice that received adenanthin treatment were maintained (Figure

5F). In summary, adenanthin serves as an effective compound that can suppress the *in vivo* growth of xenograft NSCLC tumors with minimal toxicity.

### Discussion

Although chemotherapy is the primary treatment modality for human cancers, broad adverse effects and occurrence of drug resistance are factors that significantly reduce the efficacy of these agents while severely impacting patient quality of life [21]. Pharmacologists and chemists have recently paid more attention in research concerning natural products, as they have rich structural diversity and have

## Adenanthin inhibits non-small-cell lung cancer cell growth

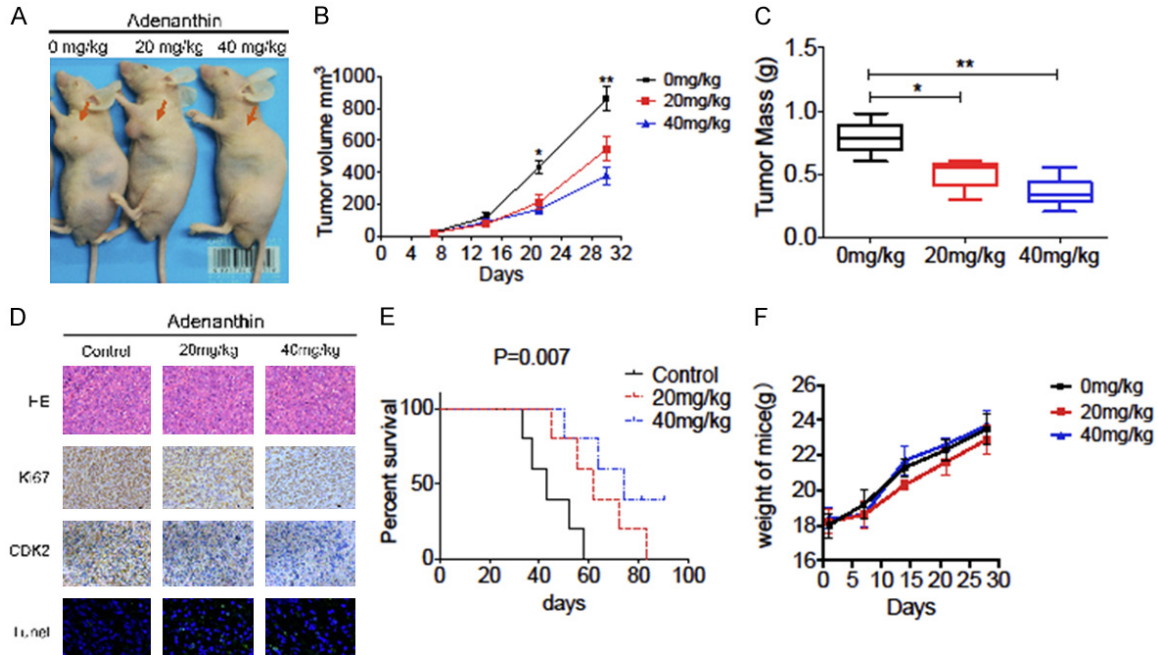


**Figure 5.** Adenanthin inhibits NSCLC cell growth *in vivo*. A, B. Balb/c nude mice were inoculated with  $2 \times 10^6$  A549 cells. Mice were grouped randomly into three cohorts ( $n = 5$ ) and given 4 weeks of daily PBS, or adenanthin at either 20 mg/kg or 40 mg/kg. A digital caliper was used to quantify tumor volumes every 3 days. B. All malignant growths were harvested from the mice after the final treatment. C. Tumor masses were weighed and contrasted with the results depicted as the mean  $\pm$  S.D. D. Tumor tissue histological characteristics were observed via H & E staining, while CDK2 and Ki67 expressions in the xenograft tumor tissues were quantified by immunohistochemistry. Apoptosis was analyzed by TUNEL assay and the percentages of TUNEL-positive were calculated with ImageJ software. E. Survival curve,  $n = 5$ . F. The body weight was measured every week.

been shown to possess promising therapeutic applications [22, 23]. This study aimed to identify medications that are novel, effective, and safe for further chemotherapeutic agent development. NSCLC cells lines H460 and A549 were demonstrated to be susceptible to adenanthin treatment, while healthy cells were spared from the compound's toxicity. Similarly, both *in vitro* and *in vivo* models of NSCLC were vulnerable to reduction in growth when exposed to adenanthin, which imparts its cytotoxic effects by triggering arrest of cell progression at the G1 phase as well as by inducing caspase-3-reliant cell death.

Cell cycle is responsible for dictating the proliferative fate of a cell and regulates complex processes that regulate cell division and growth [24]. Molecules regulating the movement of cells through this cell cycle are known as cyclins, which work by upregulating cyclin-dependent kinase (Cdk) enzymes [25]. Cells moving from the G2 to M phase are thought to be facilitated by the cyclin B1 protein [26]. The CDK2 protein also regulates cell cycle by form-

ing a key role allowing cell transition to the S phase from the G1 phase. Downregulation of both of these proteins results in arrest in the G1 cell phase [27]. Several anti-cancer compounds carry out their effects by arresting cell cycle [28, 29]. The present study found that expression of Cdc25C, Cdk2, and Cyclin B1 were attenuated in NSCLC cells (**Figure 3A, 3B**), which may indicate the occurrence of cell cycle arrest in these types of malignant cells (**Figure 3C**).

Caspases are a family of proteolytic enzymes that function to mediate apoptosis via programmed cell death. Of these, caspase-3 is an intracellular protease that is critical in apoptosis and works early in the apoptotic process [30-32]. Quantifying caspase-3 activity allows reliable and accurate assessment of apoptosis [33]. Bcl-2 proteins are also critical in mediating apoptosis. This protein family includes anti-apoptotic (e.g., Bcl-2) and pro-apoptotic (e.g., Bax) factors [34]. Anti-apoptotic protein Bcl-2 controls apoptosis by influencing caspase-3-dependent pathways [35]. With decreased

Bcl-2 and increased Bax, mitochondrion are stimulated to release cytochrome c, which in turn activates caspase-3, ultimately leading to apoptosis [34]. This study also revealed that adenanthin was able to suppress NSCLC cell growth through induction of caspase3-dependent apoptosis. After incubation with adenanthin, a dose-dependent decrease of cl-caspase3 was detected (**Figure 4D, 4E**). Moreover, the TUNEL assay, applied to test cell apoptosis in mice tumor tissues after adenanthin treatment (**Figure 5D**), revealed consistent *in vitro* results.

In summary, the current series of experiments highlight the biological mechanisms that underlie the cytotoxic effects of adenanthin in human NSCLC tumors. Both caspase3-mediated apoptosis and G1 phase cell cycle arrest were stimulated in the presence of adenanthin. Additionally, adenanthin markedly attenuated the *in vitro* and *in vivo* growth of NSCLC. Therefore, this study concludes that adenanthin may serve as a novel chemotherapeutic agent for management of NSCLC.

### Disclosure of conflict of interest

None.

**Address correspondence to:** Dr. Weiqing Li, Department of Traditional Chinese Medicine, Luohu District People's Hospital, Shenzhen, China. Tel: +86135 1082 2118; Fax: 021-51322118; E-mail: 755960096@qq.com

### References

- [1] Rebecca S, Jiemin M, Zhaohui Z and Ahmedin J. Cancer statistics, 2014. *Cancer J Clin* 2014; 64: 9-29.
- [2] Molina JR, Yang P, Cassivi SD, Schild SE and Adjei AA. Non-small cell lung cancer: epidemiology, risk factors, treatment, and survivorship. *Mayo Clin Proc* 2008; 83: 584-594.
- [3] Torre LA, Siegel RL and Jemal A. Lung cancer statistics. *Adv Exp Med Biol* 2016; 893: 1-19.
- [4] Goldstraw P, Chansky K, Crowley J, Rami-Porta R, Asamura H, Eberhardt WE, Nicholson AG, Groome P, Mitchell A, Bolejack V; International Association for the Study of Lung Cancer Staging and Prognostic Factors Committee, Advisory Boards, and Participating Institutions; International Association for the Study of Lung Cancer Staging and Prognostic Factors Committee Advisory Boards and Participating Institutions. The IASLC lung cancer staging project: proposals for revision of the TNM stage groupings in the forthcoming (eighth) edition of the TNM classification for lung cancer. *J Thorac Oncol* 2016; 11: 39-51.
- [5] Cross DA, Ashton SE, Ghiorghiu S, Eberlein C, Nebhan CA, Spitzler PJ, Orme JP, Finlay MR, Ward RA, Mellor MJ, Hughes G, Rahi A, Jacobs VN, Brewer MR, Ichihara E, Sun J, Jin H, Ballard P, Al-Kadhimi K, Rowlinson R, Klinowska T, Richmond GH, Cantarini M, Kim DW, Ranson MR and Pao W. AZD9291, an irreversible EGFR TKI, overcomes T790M-mediated resistance to EGFR inhibitors in lung cancer. *Cancer Discov* 2014; 4: 1046-1061.
- [6] Wu YL, Sequist LV, Tan EH, Geater SL, Orlov S, Zhang L, Lee KH, Tsai CM, Kato T and Barrios CH. Afatinib as first-line treatment of older patients with EGFR mutation-positive non-small-cell lung cancer: subgroup analyses of the LUX-Lung 3, LUX-Lung 6 and LUX-Lung 7 trials. *Clin Lung Cancer* 2018; 19: e465-e479.
- [7] Park M, Upton D, Blackmon M, Dixon V, Craver S, Neal D and Perkins D. Anacardic acid inhibits pancreatic cancer cell growth, and potentiates chemotherapeutic effect by chmp1A-ATM-p53 signaling pathway. *BMC Complement Altern Med* 2018; 18: 71.
- [8] Lee SI, Bae JA, Ko YS, Lee KI, Kim H, Kim KK. Geijigajakyak decoction inhibits the motility and tumorigenesis of colorectal cancer cells. *BMC Complement Altern Med* 2016; 16: 288.
- [9] Yao C, Ni Z, Gong C, Zhu X, Wang L, Xu Z, Zhou C, Li S, Zhou W, Zou C and Zhu S. Rocaglamide enhances NK cell-mediated killing of non-small cell lung cancer cells by inhibiting autophagy. *Autophagy* 2018; 14: 1831-1844.
- [10] Xu Z, Zhang F, Bai C, Yao C, Zhong H, Zou C and Chen X. Sophoridine induces apoptosis and S phase arrest via ROS-dependent JNK and ERK activation in human pancreatic cancer cells. *J Exp Clin Cancer Res* 2017; 36: 124.
- [11] Li L, Zhao SL, Yue GGL, Wong TP, Pu JX, Sun HD, Fung KP, Leung PC, Han QB, Lau CBS and Leung PS. Isodon eriocalyx and its bioactive component eriocalyxin B enhance cytotoxic and apoptotic effects of gemcitabine in pancreatic cancer. *Phytomedicine* 2018; 44: 56-64.
- [12] Siernicka M, Winiarska M, Bajor M, Firczuk M, Muchowicz A, Bobrowicz M, Fauriat C, Golab J, Olive D and Zagozdzon R. Adenanthin, a new inhibitor of thiol-dependent antioxidant enzymes, impairs the effector functions of human natural killer cells. *Immunology* 2015; 146: 173-183.
- [13] Sun HD, Huang SX and Han QB. Diterpenoids from Isodon species and their biological activities. *Natural Product Rep* 2006; 38: 673-698.

## Adenanthin inhibits non-small-cell lung cancer cell growth

- [14] Yin QQ, Liu CX, Wu YL, Wu SF, Wang Y, Zhang X, Hu XJ, Pu JX, Lu Y and Zhou HC. Preventive and therapeutic effects of adenanthin on experimental autoimmune encephalomyelitis by inhibiting NF- $\kappa$ B signaling. *J Immunol* 2013; 191: 2115-2125.
- [15] Hou JK, Huang Y, He W, Yan ZW, Fan L, Liu MH, Xiao WL, Sun HD and Chen GQ. Adenanthin targets peroxiredoxin I/II to kill hepatocellular carcinoma cells. *Cell Death Disease* 2014; 5: e1400.
- [16] Wang WG, Du X, Li XN, Yan BC, Zhou M, Wu HY, Zhan R, Dong K, Pu JX and Sun HD. Four new diterpenoids from *Isodon eriocalyx* var. *laxiflora*. *Natural Products Bioprospecting* 2013; 3: 145-149.
- [17] Hanson JR. Diterpenoids of terrestrial origin. *Natural Product Reports* 2013; 30: 1346-1356.
- [18] Yang L, Yang C, Li C, Zhao Q, Liu L, Fang X and Cheng XY. Recent advances in biosynthesis of bioactive compounds in traditional Chinese medicinal plants. *Sci Bull* 2016; 61: 3.
- [19] Zhang F, Li M, Wu X, Hu Y, Cao Y, Wang Xa, Xiang S, Li H, Jiang L, Tan Z, Lu W, Weng H, Shu Y, Gong W, Wang X, Zhang Y, Shi W, Dong P, Gu J and Liu Y. 20(S)-ginsenoside Rg3 promotes senescence and apoptosis in gallbladder cancer cells via the p53 pathway. *Drug Des Devel Ther* 2015; 9: 3969-3987.
- [20] Song X, Zhu M, Zhang F, Zhang F, Zhang Y, Hu Y, Jiang L, Hao Y, Chen S, Zhu Q, Huang W, Lu J, Gu J, Gong W, Li M and Liu Y. ZFX promotes proliferation and metastasis of pancreatic cancer cells via the MAPK pathway. *Cell Physiol Biochem* 2018; 48: 274-284.
- [21] Miao L, Guo S, Lin CM, Liu Q and Huang L. Nanoformulations for combination or cascade anticancer therapy. *Advanced drug delivery reviews* 2017; 115: 3-22.
- [22] Fang J, Cai C, Wang Q, Lin P, Zhao Z and Cheng F. Systems pharmacology-based discovery of natural products for precision oncology through targeting cancer mutated genes. *CPT Pharmacometrics Syst Pharmacol* 2017; 6: 177-187.
- [23] Fang J, Wu Z, Cai C, Wang Q, Tang Y and Cheng F. Quantitative and systems pharmacology. 1. In silico prediction of drug-target interaction of natural products enables new targeted cancer therapy. *J chem Inf Model* 2017; 57: 2657-2671.
- [24] Boeynaems S, Tompa P and Van Den Bosch L. Phasing in on the cell cycle. *Cell Division* 2018; 13: 1.
- [25] Zheng XL and Yu HG. Wnt6 contributes tumorigenesis and development of colon cancer via its effects on cell proliferation, apoptosis, cell-cycle and migration. *Oncol Lett* 2018; 16: 1163-1172.
- [26] Chikara S, Lindsey K, Dhillon H, Mamidi S, Kittilson J, Christofidou-solomidou M and reindl KM. Enterolactone induces G (1)-phase cell cycle arrest in non-small cell lung cancer cells by down-regulating cyclins and cyclin-dependent kinases. *Nutr cancer* 2017; 69: 652-662.
- [27] Wei J, Su H, Bi Y, Li J, Feng L and Sheng W. Antiproliferative effect of isorhamnetin on HeLa cells through inducing G2/M cell cycle arrest. *Exp Ther Med* 2018; 15: 3917-3923.
- [28] MarElia CB, Sharp AE, Shemwell TA, Clare Zhang Y and Burkhardt BR. Anemarrhena asphodeloides bunge and its constituent timosaponin-AIII induce cell cycle arrest and apoptosis in pancreatic cancer cells. *FEBS Open Bio* 2018; 8: 1155-1166.
- [29] Iness AN and Litovchick L. MuvB: a key to cell cycle control in ovarian cancer. *Front Oncol* 2018; 8: 223.
- [30] Juraver-Geslin HA and Durand BC. Early development of the neural plate: new roles for apoptosis and for one of its main effectors caspase-3. *Genesis* 2015; 53: 203-224.
- [31] Zhang F, Xiang S, Cao Y, Li M, Ma Q, Liang H, Li H, Ye Y, Zhang Y, Jiang L, Hu Y, Zhou J, Wang X, Zhang Y, Nie L, Liang X, Gong W and Liu Y. EIF3D promotes gallbladder cancer development by stabilizing GRK2 kinase and activating PI3K-AKT signaling pathway. *Cell Death Dis* 2017; 8: e2868.
- [32] Zhang F, Ma Q, Xu Z, Liang H, Li H, Ye Y, Xiang S, Zhang Y, Jiang L, Hu Y, Wang Z, Wang X, Zhang Y, Gong W and Liu Y. Dihydroartemisinin inhibits TCTP-dependent metastasis in gallbladder cancer. *J Exp Clin Cancer Res* 2017; 36: 68.
- [33] Min X, Heng H, Yu HL, Dan M, Jie C, Zeng Y, Ning H, Liu ZG, Wang ZY, Lin W. Anticancer effects of 10-hydroxycamptothecin induce apoptosis of human osteosarcoma through activating caspase-3, p53 and cytochrome c pathways. *Oncol Lett* 2018; 15: 2459-2464.
- [34] Campbell KJ and Tait SWG. Targeting BCL-2 regulated apoptosis in cancer. *Open Biology* 2018; 8: 180002.
- [35] Kale J, Osterlund EJ and Andrews DW. BCL-2 family proteins: changing partners in the dance towards death. *Cell Death Differ* 2018; 25: 65-80.

# Adenanthin inhibits non-small-cell lung cancer cell growth

## Supplementary Material and Method

HepG2, SGC-7901, SGC-996, PC3, cells were maintained in RPMI-1640 (Gibco, NY, USA) containing with 100 U/mL penicillin-streptomycin (Hyclone, UT, USA) and 10% fetal bovine serum (Gibco), MGC-803, Hela, HCT116, 293T, HL-7702, cells were cultured in DMEM medium (Gibco) containing 10% FBS. FHC, GES-1, IOSE144 cells were cultured in DMEM medium (Gibco) containing 10% FBS and 1% epidermal growth factor. HPDE cells were cultured in K-SFM medium (Gibco) containing 10% FBS and 1% epidermal growth factor. All cell lines were maintained at cell culture incubator with 37°C and 5% CO<sub>2</sub>.